ChemComm

Chemical Communications

www.rsc.org/chemcomm

Volume 49 | Number 21 | 14 March 2013 | Pages 2073–2162

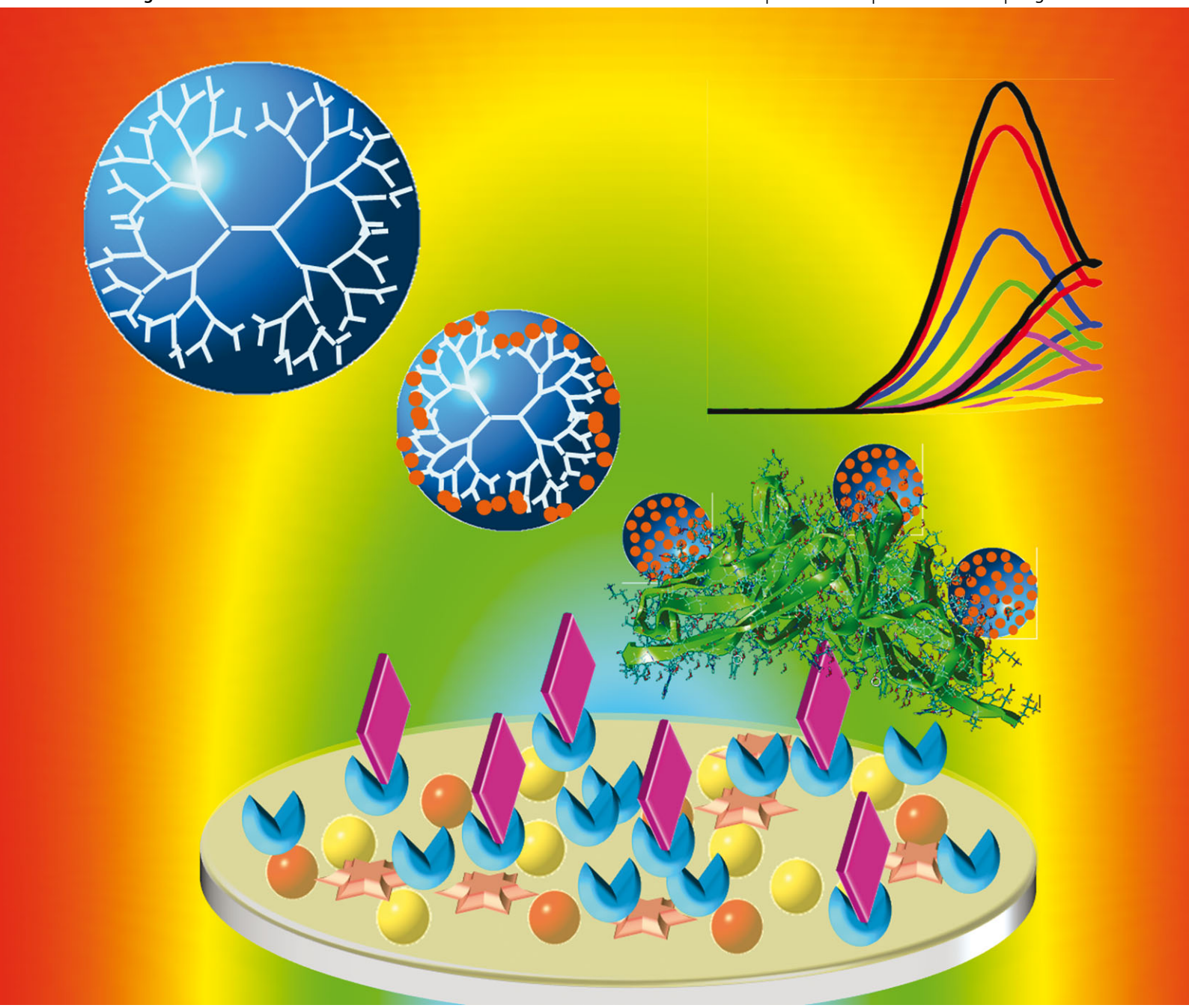

ISSN 1359-7345

RSC Publishing

COMMUNICATION

Huangxian Ju *et al.*

A ferrocenyl-terminated dendrimer as an efficient quencher *via* electron and energy transfer for cathodic electrochemiluminescent bioanalysis

ChemComm

RSC Publishing

COMMUNICATION

A ferrocenyl-terminated dendrimer as an efficient quencher *via* electron and energy transfer for cathodic electrochemiluminescent bioanalysis†

Cite this: *Chem. Commun.*, 2013, **49**, 2106

Received 26th December 2012, Accepted 28th January 2013

DOI: 10.1039/c3cc39208b

www.rsc.org/chemcomm

Shengyuan Deng, Jianping Lei, Ye Liu, Yin Huang and Huangxian Ju*

A novel ferrocenyl-terminated dendrimer with an electron-relay framework was designed as an efficient tracing tag to quench the cathodic electrochemiluminescence emission of quantum dots, which led to a dual quenching effect *via* both electron and energy transfer for construction of a sensitive bioanalysis strategy.

Quantum dot (QD)-based electrochemiluminescent (ECL) immunoassay has been rapidly developed owing to its intrinsic low background and high sensitivity.[1] Recently, two primary methodologies have been designed: steric hindrance resulting from the formation of an immunocomplex to block the mass transfer of a coreactant, and coreactant consumption with a reaction catalyzed by an enzyme-linked probe.[1] Owing to the similar nature of the QD-based ECL emission and photoluminescence (PL), energy transfer has been considered for the design of new QD-based ECL analytical methodologies.[1,2] For example, a facile strategy for the quantitative detection of β2M expressed SMMC-7721 cells has been proposed based on the resonance energy transfer between CdS QD donors and $Ru(bpy)_3^{2+}$ acceptors labelled on a cell surface.[2b] However, the QD-based energy transfer has not been applied in ECL immunoassay due to the relatively low energy transfer efficiency through the long distance between the ECL luminophore and the acceptor,[3] and the electron transfer between QDs and analyte-dependent probe has not been reported in ECL analysis yet.

Ferrocene (Fc) is a quencher of the QD-based PL emission through both energy transfer and photoexcited electron transfer.[4] It has been used for ECL detection of DNA *via* the electron transfer from the excited $Ru(bpy)_3^{2+}$.[5] Here, the electron transfer from electrochemically reduced QDs to the oxidized Fc (ferrocenium, Fc^+) was demonstrated to be capable of quenching the ECL emission of QDs. By coupling the electron-transfer mechanism with the energy transfer from excited QDs to the cyclopentadiene of Fc,[4] a dual quenching effect on QD-based ECL emission was proposed for ECL bioanalysis.

Fc can be conveniently incorporated into dendrimers, peptides, and polysaccharides for assembly of organometallic frameworks.[6] The assembled Fc moieties produce nanoscale electron delocalization among the cyclopentadienes. In order to amplify the electron transfer-based quenching effect, in this work we assembled a Fc-terminated framework by covalently binding ferrocenecarboxaldehyde (Fc-CHO) to the primary amine group of the generation-4.0 poly(amidoamine) (PAMAM) dendrimer. The designed Fc@PAMAM could be used to label biomolecules such as signal antibody (Ab_2) by the remaining amine group. Thus a tracing tag (Ab_2-Fc@PAMAM) for immunoassay was prepared, which produced a novel ECL immunosensing strategy by the dual quenching effect of Fc on QD-based ECL emission (Scheme 1).

Fc@PAMAM was facilely synthesized *via* an imine-forming amine–aldehyde reaction[7] (Scheme S1, steps a and b in ESI†) and further covalently cross-linked with Ab_2. The preparation process of the tracing tag could be confirmed by attenuated total reflection FT-IR spectra (Fig. 1A). The spectrum of Fc-CHO featured peaks of the aldehyde group at 1675 and 3088 cm^{-1} (Fig. 1A, curve a), which were attributed to C═O and C–H stretching vibrations, respectively.[6] The transmittance peaks for C═O stretching (amide I) and N–H bending/C–N stretching

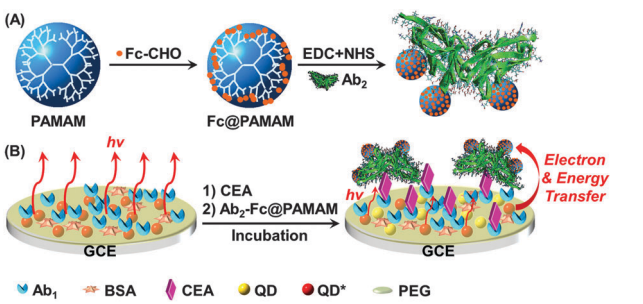

Scheme 1 Schematic illustration of (A) preparation of Fc@PAMAM-labeled antibody and (B) quenching strategy of QD-based ECL immunoassay *via* the electron and energy transfer.

State Key Laboratory of Analytical Chemistry for Life Science, School of Chemistry and Chemical Engineering, Nanjing University, Nanjing 210093, P. R. China. E-mail: hxju@nju.edu.cn

† Electronic supplementary information (ESI) available: Experimental details, morphology characterization, quenching mechanisms, optimal conditions and sensing performance. See DOI: 10.1039/c3cc39208b

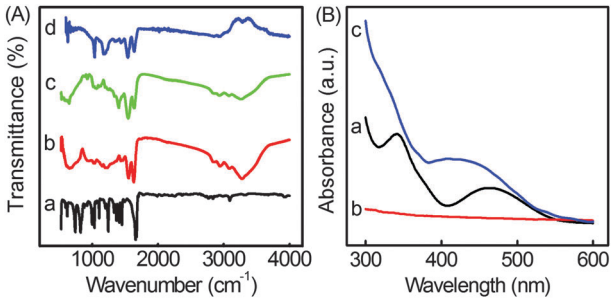

Fig. 1 (A) ATR-FTIR spectra of Fc-CHO (a), PAMAM (b), Fc@PAMAM (c) and Fc@PAMAM-labeled Ab_2 (d). (B) UV-vis absorption spectra of Fc-CHO (a), PAMAM (b) and Fc@PAMAM (c).

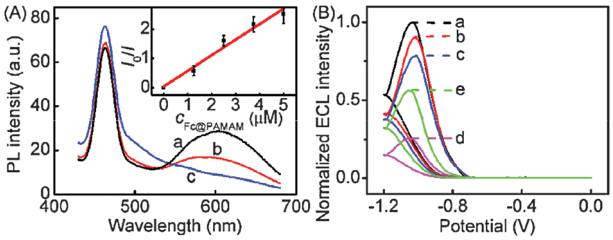

Fig. 2 (A) PL spectra of DMSA-CdTe QDs (a), (a) + 5 μM Fc-CHO (b) and (a) + 5 μM Fc@PAMAM (c). Inset in A: dependence of ECL intensity at QD modified GCE on Fc@PAMAM concentration. (B) ECL responses of QDs/PEG/Ab_1 (a), (a) incubated with 0.5 ng mL^{-1} CEA (b), and subsequently incubated with Ab_2-PAMAM (c), Ab_2-Fc@PAMAM (d) and Ab_2-Fc@PAMAM/β-CD (e) in 0.1 M pH 8.0 air-saturated PBS.

(amide II) vibrations of PAMAM dendrimers were at 1632 and 1553 cm^{-1} (Fig. 1A, curve b).[8] The broad transmittance band at 3271 cm^{-1} was assigned to the N–H stretching mode of the terminal amine group. After the incorporation of Fc into dendritic molecules, the peaks for amide II were relatively stronger than those for free PAMAM (Fig. 1A, curve c), indicating the formation of C–N binding between ferrocenyl and PAMAM.[8b,c] The assembly was also verified by the atomic force microscopic (AFM) images (Fig. S1 in ESI†). After Fc-CHO was tethered, the upper limit of the scale bar grew from 5 nm up to 6 nm due to the extended branch-like conformation.

After the imine-forming amine–aldehyde reaction with a stoichiometric PAMAM/Fc ratio of 1/90, the survey scan of the X-ray photoelectron spectrum confirmed that the relative percentage of atomic concentrations was 65.36% (C1s), 11.29% (N1s), 21.95% (O1s), and 1.40% (Fe2p), respectively. As the formula for PAMAM is $C_{622}H_{1248}N_{250}O_{124}$, the average ratio of Fe/N of Fc@PAMAM was estimated to be 31/64, which was close to one half of that of the total terminal amine groups due to the steric hindrance by the conjugated ferrocenyl groups. After the binding reaction with Ab_2, the product showed a broad coupling of O–H at ~3030 cm^{-1} (Fig. 1A, curve d), confirming the successful labelling of Fc@PAMAM on Ab_2.

Fc-CHO in methanol solution exhibited two main absorption peaks at 469 and 342 nm (Fig. 1B, curve a), which were attributed to ferrocenyl groups.[9] Compared with the spectrum of PAMAM (Fig. 1B, curve b), that of Fc@PAMAM showed increasing absorbance and two broad absorption peaks corresponding to ferrocenyl groups (Fig. 1B, curve d). These peaks were wider than those for Fc-CHO with hypochromic shifts, indicating that the proximal ferrocenyls delocalized charge distribution.[8a,10]

Bidentate-chelating CdTe QDs stabilized with *meso*-2,3-dimercaptosuccinic acid (DMSA) were employed for ECL emission. The PL spectrum of the QDs displayed two peaks at 463 and 604 nm (λ_{ex} = 400 nm) (Fig. 2A, curve a). The peak at shorter wavelength approximated the inflection point of UV-vis absorption, indicating the band-gap emission of the core, while the red-shifted strong emission was derived from the surface states.[9] Obviously, the PL emission at longer wavelength was annihilated after the introduction of 5.0 μM Fc-CHO (Fig. 2A, curve b) or Fc@PAMAM (Fig. 2A, curve c). The quenching efficiency of Fc@PAMAM was estimated to be 93%, which is larger than that (56%) of Fc-CHO due to the delocalized charge distribution and a higher amount of Fc in the framework.

The QD modified glassy carbon electrode (GCE) showed an efficient cathodic ECL emission in air-saturated pH 8.0 PBS with an emission peak at −1.03 V with the dissolved O_2 as the endogenous coreactant. Upon successive addition of Fc@PAMAM into the detection solution, the ECL emission was quenched. The ratio of the initial ECL intensity (I_0) to the intensity I at a given concentration of Fc@PAMAM (I_0/I) was proportional to the concentration of Fc@PAMAM (Fig. 2A, inset), following the Stern–Volmer equation:[2b,5b]

$$I_0/I = 1 + K_{sv}\,[\text{Fc@PAMAM}]$$

where K_{sv} is the Stern–Volmer quenching constant. The K_{sv} value was estimated to be 5.31×10^6 M^{-1} (R^2 = 0.997), comparative to the value of 5.31×10^6 M^{-1} for the quenching effect of Fc on the ECL emission of $Ru(bpy)_3^{2+}$ *via* the electron transfer.[5a] The ECL emission was previously verified to be originating from the surface traps,[9] which led to a shortened distance for electron hopping and thus facilitated the effective electron transfer from the electron-injected QDs ($QD^{\bullet -}$) to the oxidation product of Fc@PAMAM (eqn (S1)–(S6) in ESI†). Here the oxidation product was formed by the reaction between $OH^{\bullet}$ and Fc@PAMAM, and not by the electrochemical oxidation of Fc@PAMAM at a potential of +0.35 V (Fig. S2 in ESI†). Thus not only the electron transfer but also the consumption of $OH^{\bullet}$ that was a reactant to form hole-injected QDs ($QD^{\bullet +}$) quenched the ECL emission.

To clarify the mechanism, β-cyclodextrin (β-CD) was utilized as a non-electroactive shield to enwrap Fc. This process was performed on an QD-based immunosensor surface by the sandwich immunoreactions with Ab_2-Fc@PAMAM (Scheme 1) and host–guest supramolecular assembly (Scheme S1, step c in ESI†) followed.[4] The immunosensor was stabilized with a polyethylene glycol (PEG) membrane,[11] which did not change the ECL intensity of QDs/GCE due to its good permeability for the coreactant. The steric hindrance from the formation of an immunocomplex with 0.5 ng mL^{-1} antigen and the subsequent PAMAM-labeled Ab_2 decreased the ECL emission by 9.9% and 21.7%, respectively (Fig. 2B, curves a–c). However, when the PAMAM-labeled Ab_2 was replaced with Ab_2-Fc@PAMAM, the ECL intensity decreased by 86.1% (Fig. 2B, curve d). Obviously, the decrease in ECL emission resulted from the quenching effect of Fc. After ferrocenyl was embedded within the cave of β-CD, the ECL intensity of the sandwich-type immunosensor

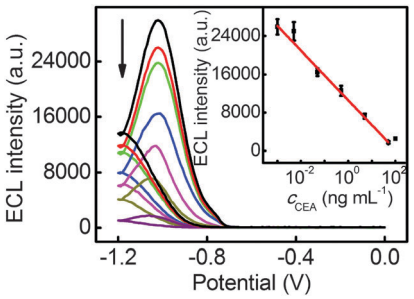

Fig. 3 ECL response of the immunosensor to 0, 0.001, 0.005, 0.05, 0.5, 5 and 50 ng mL^{-1} CEA (from top to bottom). Inset: calibration curve.

restored to about 56.3% of its initial value (Fig. 2B, curve e). This phenomenon was attributed to the incorporation of ferrocenyl into β-CD to inhibit the electron transfer between $QD^{\bullet -}$ and Fc^{+} as well as $OH^{\bullet}$ and Fc. Besides the different steric hindrances of PAMAM-labeled Ab_2 and Ab_2-Fc@PAMAM, the difference between the decreases of 21.7% and 56.3% could be attributed to the energy transfer from excited QDs (QD*) to the cyclopentadiene of Fc in Fc@PAMAM.[4] The dual quenching effect on QD-based ECL emission *via* both electron and energy transfer could improve the sensitivity of the proposed ECL bioanalysis.

Under the optimal detection conditions of pH 8.0 and 35 min incubation (Fig. S3 in ESI†), the ECL intensity of the immunosensor decreased with the increasing concentration of carcinoembryonic antigen (CEA) as a model analyte (Fig. 3). The calibration plot showed a good linear relationship between the ECL peak intensity and the logarithmic value of CEA concentration ranging from 5 pg mL^{-1} to 50 ng mL^{-1} with a correlation coefficient of 0.994 (Fig. 3, inset). The detection limit was 0.82 pg mL^{-1} at a signal-to-noise ratio of 3, which was lower than 1.4 pg mL^{-1} obtained by electrochemical immunoassay using horseradish peroxidase-functionalized carbon nanotubes as tracing labels.[12] More importantly, the immunoassay process avoided deoxygenation and the introduction of an exogenous coreactant. The wide detection range extended its practical application.

The proposed method showed good precision, acceptable reproducibility and excellent stability (Fig. S4 in ESI†). Its reliability was evaluated to be acceptable by comparing the assay results of clinical serum samples with reference values obtained from commercial ECL single-analyte tests (Table S1 in ESI†). The wider linear range spanning a positive threshold of 5 ng mL^{-1} for CEA[13] and a lower detection limit over conventional techniques, and the excellent analytical performance indicated that the proposed method possessed good practicability in clinical medicine.

A dual quenching effect on the ECL emission of QDs *via* both electron and energy transfer was demonstrated using an organometallic framework as a quencher. The ECL quencher was designed by covalently linking Fc-CHO to a primary amine group of the PAMAM dendrimer. The assembled Fc moieties showed electron delocalization among the cyclopentadiene groups, which accelerated the electron transfer from Fc to $OH^{\bullet}$ and electron-injected QDs into the oxidation product of Fc. The energy transfer from excited QDs to the cyclopentadiene of Fc further quenched the ECL emission. The residual terminal amines endowed Fc@PAMAM with aqueous dispersion and favoured further biofunctionalization with proteins. Thus a novel immunosensing strategy was proposed for ECL immunoassay with Ab_2-Fc@PAMAM as a tracing tag. This method showed a low detection limit, a wide calibration range striding over the threshold for clinical diagnosis, excellent stability, good precision, acceptable reproducibility and reliability, indicating promising practicability of the dual quenching effect.

This work was financially supported by the National Basic Research Program of China (2010CB732400), and National Natural Science Foundation of China (21121091, 21135002).

Notes and references

1 S. Y. Deng and H. X. Ju, *Analyst*, 2013, **138**, 43–61.
2 (*a*) X. Liu, H. Jiang, J. P. Lei and H. X. Ju, *Anal. Chem.*, 2007, **79**, 8055–8060; (*b*) M. S. Wu, H. W. Shi, J. J. Xu and H. Y. Chen, *Chem. Commun.*, 2011, **47**, 7752–7754.
3 W. Yao, L. Wang, H. Y. Wang, X. L. Zhang, L. Li, N. Zhang, L. Pan and N. N. Xing, *Biosens. Bioelectron.*, 2013, **40**, 356–361.
4 D. Dorokhin, S. H. Hsu, N. Tomczak, D. N. Reinhoudt, J. Huskens, A. H. Velders and G. J. Vancso, *ACS Nano*, 2010, **4**, 137–142.
5 (*a*) W. D. Cao, J. P. Ferrance, J. Demas and J. P. Landers, *J. Am. Chem. Soc.*, 2006, **128**, 7572–7578; (*b*) W. Cao, J. Ferrance, J. Demas and J. P. Landers, *J. Am. Chem. Soc.*, 2006, **128**, 7572–7578; (*c*) A. E. Radi, J. L. A. Sánchez, E. Baldrich and C. K. Sullivan, *J. Am. Chem. Soc.*, 2006, **128**, 117–124.
6 (*a*) B. Fabre, *Acc. Chem. Res.*, 2010, **43**, 1509–1518; (*b*) T. Moriuchi and T. Hirao, *Acc. Chem. Res.*, 2010, **43**, 1040–1051.
7 J. Das, Md. A. Aziz and H. Yang, *J. Am. Chem. Soc.*, 2006, **128**, 16022–16023.
8 (*a*) D. Astruc, *Nat. Chem.*, 2012, **4**, 255–267; (*b*) J. Satija, V. V. R. Sai and S. Mukherji, *J. Mater. Chem.*, 2011, **21**, 14367–14386; (*c*) G. Franc and A. K. Kakkar, *Chem. Soc. Rev.*, 2010, **39**, 1536–1544.
9 X. Liu, L. X. Cheng, J. P. Lei, H. Liu and H. X. Ju, *Chem.–Eur. J.*, 2010, **16**, 10764–10770.
10 (*a*) Y. Ochi, M. Suzuki, T. Imaoka, M. Murata, H. Nishihara, Y. Einaga and K. Yamamoto, *J. Am. Chem. Soc.*, 2010, **132**, 5061–5069; (*b*) A. F. Wang, C. Ornelas, D. Astruc and P. Hapiot, *J. Am. Chem. Soc.*, 2009, **131**, 6652–6653.
11 J. A. Ho, H. C. Chang, N. Y. Shih, L. C. Wu, Y. F. Chang, C. C. Chen and C. Chou, *Anal. Chem.*, 2010, **82**, 5944–5950.
12 V. Mani, B. V. Chikkaveeraiah, V. Patel, J. S. Gutkind and J. F. Rusling, *ACS Nano*, 2009, **3**, 585–594.
13 S. Ishigami, S. Natsugoe, S. Hokita, X. M. Che, K. Tokuda, A. Nakajo and H. Iwashige, *J. Clin. Gastroenterol.*, 2001, **1**, 41–44.

